



Fall 2022

Gulf of Mexico Health & Air Quality II
Mapping Methane Emission Plumes Using Sunlint-configured Imagery for
Monitoring Offshore Oil & Gas Activity

DEVELOP Technical Report

Final – November 18th, 2022

Ben Dahan (Project Lead)
Vanessa Machuca
René Castillo
Melodi Hess

Advisors:

Dan Cusworth, Carbon Mapper, NASA Jet Propulsion Laboratory; University of Arizona (Science Advisor)
Kate Howell, Carbon Mapper (Science Advisor)
Ben Holt, NASA Jet Propulsion Laboratory (Science Advisor)

Previous Contributors:

Kate Howell
Ashley Fernando
Ephrata Yohannes
J. Kyle Bergerson

Fellow:

Kathleen Lange (JPL)

1. Abstract

Offshore oil and gas production in the United States is a major source of anthropogenic greenhouse gas emissions and accounts for nearly 30% of global oil and gas production. Methane venting and flaring are primary contributors to offshore emissions, and monitoring these activities is crucial for mitigating greenhouse gas emissions. Limited ground truthing and intermittent offshore satellite revisits make monitoring venting and flaring challenging. The Bureau of Ocean Energy Management (BOEM) and the Bureau of Safety and Environmental Enforcement (BSEE) oversee offshore oil and gas activity but rely primarily on operator-reported data. The non-profit organization SkyTruth monitors natural resources like methane and identifies sources of fugitive emissions. By combining BOEM and BSEE's operational data along with observations from Sentinel-2 Multispectral Instrument (MSI), Landsat 8 Operational Land Imager (OLI) and Landsat 9 OLI-2, and PRecursore IperSpettrale della Missione Applicativa (PRISMA), the team further identified ultra-emitter point sources in the Gulf of Mexico using sunglint-configured imagery. We quantified these plume emission rates using the methodology from Varon et al. (2020). The team found three plumes in the Gulf of Mexico occurring between 2020 and 2022 using Sentinel-2 MSI and Landsat 9 OLI-2 imagery, in addition to the single plume identified by the Gulf of Mexico Health & Air Quality I team, and successfully quantified three plumes. Our statistical retrieval of three PRISMA images tasked over areas of interest yielded no methane plumes, despite a successful test of a known plume in Assam, India. These analyses serve as a proof of concept for the utility of remote sensing for methane emission monitoring offshore, which can complement regulator emission inventories and validate self-reported operator records.

Key Terms

sunglint, flaring, venting, methane plumes, Landsat 8 OLI, Landsat 9 OLI-2, Sentinel-2 MSI, PRISMA

2. Introduction

2.1 Background Information

Offshore oil and gas production in the Gulf of Mexico (Figure 1) is a multi-billion-dollar industry and accounts for nearly 15% of the total crude oil production in the United States (Bureau of Ocean Energy Management Outer Continental Shelf 2022). Despite the undergoing transition to renewable energy, the offshore oil industry is forecasted to experience robust growth and record high total oil production in the coming years (Short-Term Energy Outlook [STEO], 2019). As major global oil and gas companies invest heavily in offshore production, it is important to recognize the contributions that these operations make to coastal air quality degradation and anthropogenic climate change (Cenovus Energy, Inc., 2021; Equinor ASA, 2019).



Figure 1. Study area map of U.S. Federal waters in the Gulf of Mexico.

In the extraction of fossil fuels, offshore facilities produce extraneous gases like methane (CH_4) which must be safely dispelled by either venting or flaring. These gasses may be “flared”—which burns off excess CH_4 but releases carbon dioxide (CO_2), nitrous oxide (NO_2), and water vapor (H_2O)—or “cold-vented”, which vents CH_4 directly into the atmosphere. Even when the gases are flared, unlit flares and inefficient combustion destroy only 91% of methane, much lower than the 98% efficiency some operators claim, which results in a fivefold increase in global methane emissions than under current assumptions (Plant et al., 2022). The radiative forcing of CH_4 is 84 times that of CO_2 within the molecule’s lifespan in the atmosphere and CH_4 accounts for a quarter of global warming from anthropogenic greenhouse gas gases since the Industrial

Revolution (Kirschke et al., 2013). While monitoring these emissions in the Gulf of Mexico is critical to meeting global methane reduction targets and mitigating environmental damage, no systemic practices currently exist to validate operator self-reported data for venting and flaring. Moreover, the studies conducted for both onshore and offshore facilities have consistently found discrepancies between facility reported CH₄ inventories, *in situ* measurements, and remotely sensed measurements (Gorchov Negron et al., 2020; Xiao et al., 2008; Ayasse et al., 2022).

The uncertainty surrounding CH₄ emission in the Gulf of Mexico cannot be explicated using a bottom-up monitoring approach. In order to strengthen the confidence of emission estimates, a top-down monitoring approach using satellite imagery is necessary. Varon et al. (2021) presented three methods for using shortwave infrared (SWIR) measurements from multispectral satellites, specifically Sentinel-2, to capture methane plumes and derive source rates. Cusworth et al. (2020) further demonstrated the utility of combining multiple satellite data sources, including hyperspectral sources, to identify and quantify methane plumes. However, both papers deal with high-emission events onshore. Offshore methane retrievals are more difficult to execute due to the reflective signature of ocean water, particularly its high absorption of SWIR radiation, and requires solar radiation to be reflected by the water surface in a phenomenon called sunglint. Several studies, such as Ayasse et al. (2022), demonstrate the feasibility of using airborne sensors and sunglint to capture methane plumes, while Irakulis-Loitxate et al. (2022) chronicled an ultra-emissions event using the high-resolution WorldView-3 satellite. This study adapts the existing multispectral methodology from Varon et al. (2021) and the hyperspectral methodology from Cusworth et al. (2020) to locate and quantify sunglint-illuminated methane plumes using satellite imagery derived from NASA Earth observation satellite Landsat 8 and Operational Land Imager (OLI) and Landsat 9 OLI-2, the European Space Agency's Copernicus Sentinel-2 Multi Spectral Instrument (MSI), as well as the Italian Space Agency's PRercursores IperSpettrale della Missione Applicativa (PRISMA) satellite.

This study builds on the work of the Gulf of Mexico Health & Air Quality I team that used Suomi National Polar-orbiting Partnership Visible Infrared Imaging Radiometer Suite (NPP VIIRS) Nightfire imagery to validate operator-reported flaring in the Gulf of Mexico and identify oil and gas platforms in additional areas of interest. The Gulf of Mexico Health & Air Quality I team additionally utilized sunglint to illuminate methane plumes over offshore oil and gas platforms using Sentinel-2 MSI from 2017 to 2019. Using this method, they were able to detect two potential methane plumes in the Gulf of Mexico and off the Coast of Lagos. This project focused on locating and quantifying methane plumes in the Gulf of Mexico from 2020 through 2022.

2.2 Project Partners & Objectives

The Bureau of Ocean Energy Management (BOEM) has a statutory requirement in the Outer Continental Shelf Lands Act (OCSLA) and in the National Environmental Policy Act (NEPA) to perform air quality impact assessments of leasing program activities. BOEM's mandate from the Clean Air Act focuses on criteria pollutants, but the agency may soon begin issuing regulations on greenhouse gas emissions within its jurisdiction in the Gulf of Mexico (BOEM, n.d). Its sister agency—the Bureau of Safety and Environmental Enforcement (BSEE)—enforces BOEM's rulemaking, and regulates venting and flaring activity (BSEE, n.d). The non-profit SkyTruth monitors natural resources and pollutants, including methane emissions. Monitoring traditionally occurs through bottom-up assessments from self-reported emission inventories, with occasional inspections using infrared cameras to identify fugitive emissions. These data do not reflect the length of time or quantity of methane emitted. There are currently no offshore monitors. Therefore, BOEM and BSEE have an interest in increasing their monitoring capacity of offshore oil and gas operations through remote sensing. To support our partners in this effort, this project identified methane plumes from venting and flaring activities in the Gulf of Mexico by using sunglint-configured images and derived an estimated emission rate for identified plumes. This research will increase BOEM and BSEE's understanding of emissions in the Gulf of Mexico and demonstrate potential methodologies to incorporate remote sensing into their regulatory activities.

3. Methodology

3.1 Data Acquisition

We downloaded Sentinel-2 MSI and Landsat 8 and 9 OLI images from Earth Engine Data Catalog through the Google Earth Engine (GEE) Python API. Our science advisor, Dan Cusworth, procured three PRISMA images from the Italian Space Agency. One PRISMA image was captured over the Gulf of Mexico on June 21, 2022, and two other images off the coast of South America on September 3rd and 4th, 2022. Earth observation products and parameters are provided in Table 1. BOEM provided a dataset consisting of 2021 flaring and venting volumes per platforms and platform locations. Additionally, Dan Cusworth provided access to the Dark Sky weather reanalysis products that derive wind speed and wind direction for the target locations. Another science advisor for the project, Benjamin Holt, provided the team with four high resolution images from Planet to use for manual visual analysis and to compare plumes to the plume emission sources. These Planet images were acquired through NASA’s Commercial Smallsat Data Acquisition program. Our partners provided us with oil and gas platform data, including the currently-unpublished 2021 emissions inventory, daily operator venting and flaring volume records, and platform schematics.

Table 1

Satellites and sensors used in this project.

Platform & Sensor	Products	Parameters
Sentinel-2 MSI	Harmonized Level-1C Top of Atmosphere Reflectance	Red, green, and blue bands SWIR1 and SWIR2 bands Cloudy pixel percentage QA60 cloud mask
Landsat 8 OLI	Collection 2 Tier 1 TOA reflectance	SWIR1 and SWIR2 bands QA cloud filter
Landsat 9 OLI-2	Collection 2 Tier 1 TOA reflectance	SWIR1 and SWIR2 bands QA cloud filter
PRISMA	N/A	SWIR Visible and Near Infrared (VNIR)
PlanetScope	N/A	Visual comparison and analysis

3.2 Data Processing

Prior to the sunglint methane analysis, Sentinel-2 and Landsat 8 and 9 imagery were pre-processed by filtering to remove any images with a cloudy pixel percentage greater than 15%. This threshold was selected to remain consistent with the methodology of Varon et al., 2021. The Sentinel-2 imagery was filtered by individual cloudy pixels using the QA60 cloud mask. We filtered Landsat 8 and 9 OLI imagery using the quality assurance (QA) filter to produce the cloud and shadow mask. To select images containing sunglint, the imagery was masked by SWIR (Sentinel-2 band 11 and Landsat 8 and 9 band 6) reflectance values greater than 0.13. We inspected the images with sunglint present in GEE to determine a visual threshold for the reflectance value threshold, then calculated the percentage of sunglint pixels in each image with the reflectance mask and chose images with a sunglint percentage greater than 20% for further analysis.

3.3 Data Analysis

3.3.1 Methane Retrieval and Plume Identification

We used the methodology developed by Dan Cusworth to perform a statistical retrieval on the PRISMA images to search for methane plumes. (Cusworth et al., 2020). The PRISMA image contains both SWIR and VNIR datasets that were stitched together to form a data cube, where the mean spectra were then identified for the image and compared the spectra of the pixels containing the target platform. The difference was then used to relate the change in pixel radiance to methane concentration using a unit absorption spectrum script. Next, we ran a publicly available Python tool called MAG1C (Matched filter with Albedo correction and reweighted L1 sparsity Code) that reduces error by correcting for sparsity and albedo in the input image (Foote et al., 2020), and accounts for the change in CH₄ given the unit absorption and solar zenith angle. This process outputs a unitless value that roughly corresponds to methane presence within each pixel.

We used a multi-band-single-pass (MBSP) methodology developed by Varon et al. (2021) for the Landsat 8 and 9 OLI/OLI-2 and Sentinel-2 MSI images. This process involved comparing the signals from two SWIR bands in a single satellite pass—Sentinel-2 Band 12 and Landsat Band 7 being more sensitive to methane than Sentinel-2 Band 11 and Landsat Band 6. A large difference in signal between the bands indicates the presence of methane. This change in reflectance, ΔR , is calculated using Equation 1.

$$\Delta R = \frac{cR_a - R_b}{R_b} \quad (1)$$

where c accounts for the difference in signal output between the two bands and is calculated using a least-squares fitting between SWIR bands 11 and 12 in the Sentinel-2 images, and bands 6 and 7 in the Landsat 8 and 9 images, across the scene. R_a accounts for the bands with stronger methane absorption, and R_b accounts for the bands with weaker methane absorption. The difference in the numerator is then divided by R_b to normalize unexpected artifacts across the two bands. ΔR is then fed into Equation 2:

$$m(\Delta\Omega) = \frac{T_a(\Omega + \Delta\Omega) - T_a(\Omega)}{T_a(\Omega)} - \frac{T_b(\Omega + \Delta\Omega) - T_b(\Omega)}{T_b(\Omega)} \quad (2)$$

where T_a and T_b are the top of atmosphere (TOA) radiances for the two bands being compared, where band a exhibits a higher sensitivity to methane than band b . $\Delta\Omega$ represents methane column enhancement. Methane concentration (kg s^{-1}) is determined by minimizing this equation (Varon et al., 2021). These concentrations were mapped across subsets of the images of interest in search for methane plumes and to choose spatial subsets by using both VIIRS and BOEM 2021 draft inventory data to isolate top venters and flares in the Gulf of Mexico.

3.3.2 Emission Rate Quantification

Emissions rates were quantified from identified methane plumes from Landsat 9 OLI-2 and Sentinel-2 MSI images using Equation 3:

$$Q = \frac{IME \times U_{eff}}{L} \quad (3)$$

where integrated mass enhancement (IME) is the sum of all methane concentrations across all pixels in the plume image in meters. U_{eff} is the effective wind speed over the plume in m s^{-1} and is found by taking the 100-meter modeled wind speed from Ventusky and scaling it to account for plume dispersion. L is the size of the plume in meters., calculated by finding the square root of the plume area. This results in an emission rate Q , in units of kg s^{-1} for a plume in the instance in time the image was captured.

4. Results & Discussion

4.1 PRISMA

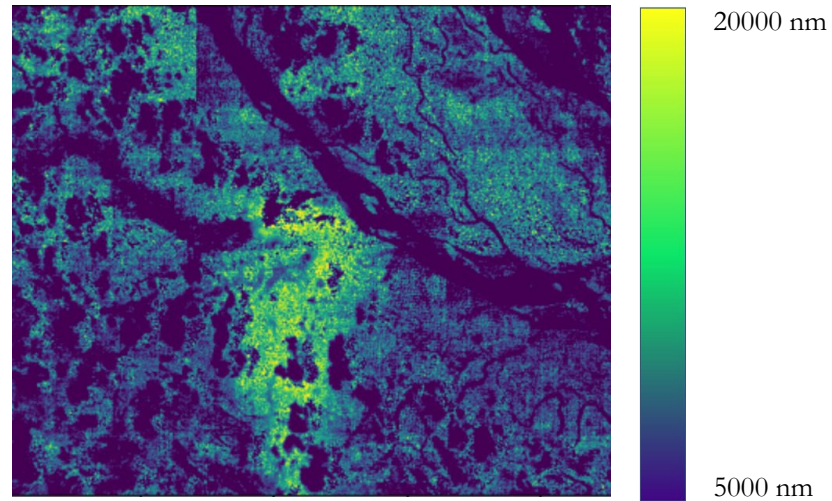


Figure 2. Statistical retrieval conducted over the Baghjan Oil Field in Assam, India. PRISMA image taken on May 31, 2020.

Figure 2 represents the Baghjan natural gas blowout, which occurred in Assam, India, in 2020. As a well-documented, high-emissions event, this is where we tested our statistical retrieval code to ensure we were correctly identifying and retrieving methane in the spectral signature of the images. While this test was successful, we were not able to identify any methane plumes offshore in the three PRISMA images we examined. This is likely due to the limited number of images we were able to procure. Given that PRISMA is a tasked satellite, it is also somewhat challenging to capture images of platforms within the duration of a venting event. However, we believe that PRISMA would be especially useful to harmonize satellite sensor methane retrievals with planned controlled release events. This would allow the retrieval algorithm to be calibrated to known, ground truthed emission volumes and rates.

4.2 Sentinel-2 and Landsat 8 and 9

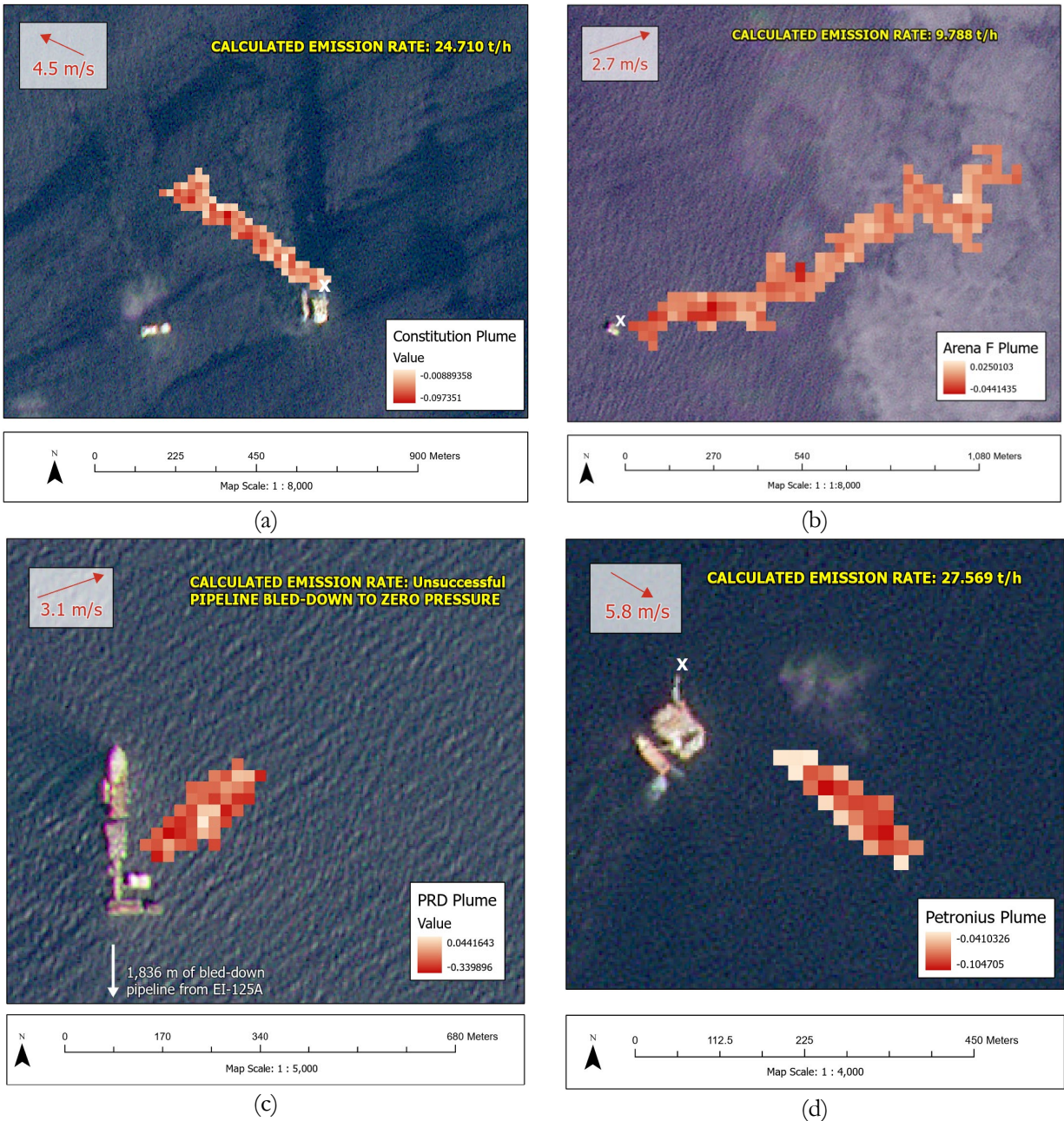


Figure 3. Plume overlays for (a) Constitution, (b) F, (c) PRD, and (d) Petronius. (a) Plume image taken by Sentinel-2 MSI on July 5, 2017, overlaid on PlanetScope image taken on August 17, 2022 at platform coordinates 27.29220815, -90.96802088. (b) Plume image taken by Landsat-9 OLI on May 16, 2022, overlaid on PlanetScope image taken on September 1, 2022, at platform coordinates 28.43025, -91.46957. (c) Plume image taken by Sentinel-2 MSI on March 16, 2022, overlaid on PlanetScope image taken on September 16, 2022 at platform coordinates 28.97905, -91.4727. (d) Plume image taken by Sentinel-2 MSI on May 7, 2021, overlaid on PlanetScope image taken on September 12, 2022 at platform coordinates 29.229, -87.781. White Xs delineate vent and flare boom location based on schematics. Red arrow delineates wind speed and direction. © Planet Labs PBC 2022. All rights reserved.

This study identified three plumes in the Gulf of Mexico across 2020 and 2022 in addition to the plume identified by the previous team. Two were identified with Sentinel-2 MSI, and the other was identified using Landsat 9 OLI-2. We were able to quantify emission rates for 3 out of the 4 plumes. The plumes are referred to by the common name of the platform each was associated with. To investigate each plume candidate, we used RGB to MBSP comparisons, wind speed and direction, and contextual information such as schematics and daily operator venting and flaring records provided by our partners. Plume masks were generated in ArcGIS Pro to extract the potential plumes from the MBSP, then overlaid on the true color Planet images (Figure 3). The Planet images were not captured at the same time the plumes were.

Figure 3a was identified in the project's first term, captured by Sentinel-2 MSI on July 5, 2017 at the Green Canyon Area, Block 680, "Constitution" platform (GC 680 "Constitution"). The RGB (Appendix B1) shows the platform and shadows from clouds that were present but outside the viewing angle of the instrument. In the MBSP image, the cloud shadows and platform still show up, but so does a trail of red extending from the platform to the northwest. There are a few pieces of compelling evidence that indicate this to be a vented methane plume. In examining higher resolution Planet images, it was found that this platform flares from the same location that this potential plume is extending from. This is a strong indication that the platform vents from that location as well. Additionally, the plume feature appears in the MBSP but not in the RGB and does not exhibit the same mirroring behavior as the cloud shadow in the MBSP. The wind was also moving northwest at 4.5 m s^{-1} , which matches the trajectory of the plume. Upon establishing that this is a likely a methane plume, the methane concentration retrieval on the MBSP image was performed to determine an emission rate. The estimated emission rate was 24.710 t h^{-1} , which is within the range of plausibility for a plume this size.

Figure 3b was captured by Landsat 9 OLI-2 on May 16th, 2022, at the Eugene Island Area, Block 276, "F" platform (EI 276 "F"). While we were able to identify a plume and retrieve methane using the MBSP (Appendix B2), this image is just within the threshold for acceptable sunglint conditions and would be more confident in our emission rate were the true color image at a higher sunglint threshold. However, the wind direction was in our favor, and we were not able to identify any features in the true color image that could set off a false positive in our MBSP, so we performed the methane concentration retrieval and estimated an emission rate of 9.630 t h^{-1} .

Figure 3c was captured on March 16, 2022, by Sentinel-2 at the Eugene Island Area, Block 120, "PRD" platform (EI 120 "PRD"). Again, the plume appears in the MBSP image and not in the RGB, indicating that it is likely not a water or cloud feature (Appendix B3). The wind was blowing to the northeast near the time this image was captured at 3.1 m s^{-1} . This plume is more dispersed than the other plumes, possibly due to the relatively low wind speed. We were unable to determine an emission rate for this plume, owing to how dispersed it is as well as how dark the image is. Though no venting or flaring activity had occurred at the time this image was captured, our partners informed us that a pipeline connecting to a nearby platform was "bled-down" to zero pressure the day prior. The MBSP is likely picking up methane released when this pipeline was emptied of its contents. Due to low sunglint, noise, and cloud cover, it is difficult to discern whether methane was dispelled from the adjoining platform as well.

Figure 3d was captured on May 7th, 2021, by Sentinel-2 MSI at the Viosca Knoll Area, Block 786, "Petronius" platform (VK 786 "Petronius"). The plume begins some distance away from the edge of the platform—around 75 meters. Our partners sent a schematic of the Petronius platform, which indicated that the venting boom extends from the northern point of the platform, which is even further from the start of the plume. However, the wind is blowing at 5.8 m s^{-1} in the same direction as the plume, so it is plausible that the vented methane was blown away from the venting boom and that this image was captured after the platform stopped venting. There are no other features in the RGB that point to some other source of this plume-like feature in the MBSP image (Appendix B4). In any case, this was a great example of stakeholder engagement in how involved our partners were in investigating this potential plume. The emission rate was estimated to be 27.569 t h^{-1} , which differs considerably from the rate calculated from operator-reported daily vented volumes but is within the range of plausibility.

4.3 Future Directions

Outlined here are several steps a future team can take to improve the accuracy for quantified methane plume emission rates. First, the atmospheric model used in quantifying methane emissions should be modified to more accurately reflect ocean environments. This could include changing the assumed surface reflectance within the radtran python script used in the analysis, which currently assumes a Lambertian surface, i.e., a diffusely reflecting or “matte” surface. Such changes will likely improve the accuracy of the resulting estimate plume emission rate. Additionally—as wind is expected to be a major source of uncertainty—a future team can explore using *in situ* wind data as opposed to modeled wind reanalysis products. Quantification accuracy can likewise be improved by filtering the plume mask to include only pixels within the plume itself. This project—with only four identified plumes—did this step manually. This process ensures that outliers and noise in the image are not incorrectly identified as methane and included in the estimated plume concentration. However—to scale the study to a large number of plumes and to automate the process—a future team should apply a Gaussian filter to smooth methane concentration images, as demonstrated in Varon et al. (2021).

A future team can expand the analysis of hyperspectral imaging, such as the PRISMA analysis. The small sample size of three PRISMA images—tasked over areas where potential plumes had been identified last term—limited the ability to capture methane emitting activities at the time the image was taken despite successfully demonstrating the method. PRISMA can be prescribed over oil and gas platforms identified in this project in coordination with planned methane-releasing activities, such as preventative maintenance. The accuracy of the statistical retrieval conducted in the images may also be improved by developing a cloud mask, which currently does not exist for PRISMA. The presence of clouds can skew statistical retrieval results in a PRISMA image as it averages pixel values across an image. Future researchers can also attempt a multi-band single-pass analysis as an alternative methodology to the statistical methane retrieval. As PRISMA has a finer spectral resolution than multispectral imagers like Sentinel-2, future teams can experiment with which combination of methane-sensitive and methane-insensitive hyperspectral bands to use (Appendix A).

Further work is also needed to expand the scope beyond the date and geographical range chosen for this study to increase the sample size of potential plumes and robustness of such methodologies. After demonstrating that Sentinel-2 MSI and Landsat 8 OLI and 9 OLI-2 are capable of detecting methane plumes from offshore oil and gas facilities, a search can include their full image collections—which date back to 2015 and 2013, respectively. This project used data from the BOEM 2021 emission inventory to prioritize oil and gas platforms known to be engaged in venting or flaring activity and assumed these same platforms would be active in 2020 and 2022. Though such self-reported and geolocated data may not be readily available in other areas of interest—such as the production-heavy coasts of Southeast Asia, South America, or West Africa—a future team could use VIIRS Nightfire from the Suomi NPP satellite to identify locations of flaring. Flaring can also produce a noticeable image artifact in an MBSP layer, which can be used to identify high-potential locations. The parameters for sunglint filtering within Google Earth Engine—the reflectance and glint image threshold—can be adjusted upwards to output fewer, more high-quality images.

Finally, a future team could build on this work to make remotely sensed methane emission more actionable for the partners’ regulatory and monitoring efforts. NASA’s real-time air quality monitoring TEMPO geostationary satellite will be launched in 2023, and its data may be made available to BOEM and BSEE for monitoring criteria pollutants. Elsewhere, low NO₂/SO₂ column density ratio has been shown to indicate flaring, such as in the last term’s project and Zhang et al. (2019). This can be compared to the methane plumes spectrally identified here, as well as self-reported disposed gas inventories, and can contribute to validating operator flaring activity.

5. Conclusions

The atmospheric concentration of methane as a result of oil and gas production is a notable contributor to anthropogenic methane budget. This project has demonstrated the practical integration of remote sensing within the oil and gas industry for greenhouse gas emissions regulation and mitigation efforts. The ability to

utilize sunglint-configured imagery to constrain methane presence within the atmosphere of the Gulf of Mexico and quantify emissions has equipped our partners with a methodology that will actively support and improve their regulatory efforts. Where emission data availability is sparse or absent, remote sensing methodologies, such as our emission identification and quantification processes, provide an additional resource to investigate the movement of methane from point source to the atmosphere.

Building upon the previous team's methods, we tested two methods for methane retrieval. The team identified additional methane plumes using sunglint-configured imagery to supplement and validate the previous term's proof of concept for this technique. Presently, the MBSP methodology most successfully leverages sunglint-configured multispectral data in offshore methane retrieval and quantification. The sparsity of hyperspectral data limits the success of a widespread implementation of the statistical retrieval method. With the future release of new hyperspectral instruments and the subsequent increase in data availability, this method will become progressively more suitable for the analysis and integration of high-resolution hyperspectral imaging within the field of remote sensing and for the purposes of offshore methane retrieval across a broader spatiotemporal scale.

These methodologies can be applied to various study areas and utilize many NASA Earth observation datasets and sensors as well as instruments manufactured by other space agencies across the world. This allows organizations like BOEM to better monitor and regulate methane emissions within their jurisdiction and study methane emissions and concentrations. The results of these analyses directly support BOEM and BSEE in accurately monitoring methane emissions and enacting regulatory compliance. This work furthers BOEM and BSEE's capacity to integrate upcoming satellite missions and remote sensing into their operations and increases their abilities in facilitating a more robust and comprehensive methane emission monitoring program.

6. Acknowledgments

The Gulf of Mexico Health and Air Quality II team would like to thank the mentors and partners who provided their support and time to make this project possible. Thank you to our science advisors Benjamin Holt, Dan Cusworth and Kate Howell for their wisdom and expertise. We owe our gratitude to Jason Schatz and the team of SkyTruth for being our collaborators, and DEVELOP Fellow Katie Lange for her enthusiasm and guidance. We would also like to thank our partners at BOEM and BSEE, Jay Cho, Ramona Sanders, Jarvis B. Abbott, Holli D. Ensz, Nellie Elguindi, Cholena Ren, Thomas Kilpatrick, and Ross Laidig for their invaluable insight and support throughout this project.

This material contains modified Copernicus Sentinel data (2019-2021), processed by ESA.

This material contains modified PRISMA data (2022), processed by ASI.

This work utilized data made available through the NASA Commercial Smallsat Data Acquisition (CSDA) program. © Planet Labs PBC 2022. All rights reserved.

Any opinions, findings, and conclusions or recommendations expressed in this material are those of the author(s) and do not necessarily reflect the views of the National Aeronautics and Space Administration.

This material is based upon work supported by NASA through contract NNL16AA05C.

7. Glossary

Earth observations – satellites and sensors that collect information about the Earth's physical, chemical, and biological systems over space and time

BOEM – Bureau of Ocean Energy Management

BSEE – Bureau of Safety and Environmental Enforcement

Flaring – Process of burning gas which, at full efficiency, releases CO₂, NO₂, and water vapor into the atmosphere

GEE – Google Earth Engine

GOM – Gulf of Mexico

IME – integrated mass enhancement

In situ observations- observations made at the point where the measuring instrument is located

MBSP – multi-band-single-pass

MSI – Multispectral Instrument

NEPA – National Environmental Policy Act

NPP VIIRS - National Polar-orbiting Partnership Visible Infrared Imaging Radiometer Suite

OCSLA – Outer Continental Shelf Lands Act

OLI – Operational Land Imager

PRISMA – *PR*ecursore *I*perSpettrale della *M*issione *A*pplicativa

QA – quality assurance

Remote sensing – science of obtaining information about objects or areas from a distance, typically from aircraft or satellites

SWIR – Short wave Infrared

Revisit Time – denotes how frequently data of the same area is collected

TOA – top of atmosphere

Venting – Direct release of methane gas into the atmosphere

VNIR – visible and near infrared

8. References

- Ayasse, A. K., Thorpe, A. K., Cusworth, D. H., Kort, E. A, Gorchov Negron, A., Heckler, J., Asner, G., Duren, R. M.,(2022). Methane remote sensing and emission quantification of offshore shallow water oil and gas platforms in the Gulf of Mexico. *Environmental Research Letters*, 17, Article Number [084039]. <https://iopscience.iop.org/article/10.1088/1748-9326/ac8566>
- BOEM *Governing* Statutes. U.S. Department of The Interior BOEM Bureau of Ocean Energy Management. <https://www.boem.gov/about-boem/regulations-guidance/boem-governing-statutes#:~:text=The%20most%20important%20legislation%20for%20BOEM%20is%20the,of%20its%20offshore%20mineral%20resources%20and%20energy%20resources>
- BP. (2022, May). *Newfoundland & Labrador Orphan Basin exploration drilling project*. BP Canada. https://www.bp.com/en_ca/canada/home.html
- BSEE National Programs. U.S. Department of The Interior BSEE Bureau of Safety and Environmental Enforcement. <https://www.bsee.gov/about-bsee/our-organization/national-programs>
- Copernicus Sentinel data processed by ESA, Koninklijk Nederlands Meteorologisch Instituut (KNMI) (2021), Sentinel-5P TROPOMI Tropospheric NO₂ 1-Orbit L2 5.5km x 3.5km, Greenbelt, MD, USA, Goddard Earth Sciences Data and Information Services Center (GES DISC), Accessed: October 5 2022, <https://doi.org/10.5270/S5P-9bnp8q8>
- Copernicus Sentinel data processed by ESA, German Aerospace Center (DLR) (2020), Sentinel-5P TROPOMI Sulphur Dioxide SO₂ 1-Orbit L2 5.5km x 3.5km, Greenbelt, MD, USA, Goddard Earth Sciences Data and Information Services Center (GES DISC), Accessed: October 5 2022, <https://doi.org/10.5270/S5P-74eidii>
- Copernicus Sentinel data (2022), Sentinel-2 MSI: Multispectral Instrument Level 1-C. Accessed: October 5 2022, developers.google.com/earth-engine/datasets/catalog/COPERNICUS_S2_HARMONIZED?hl=en

- Cusworth, D. H., Duren, R. M., Thrope, A. K., Pandey, S., Maasackers, J. D., Aben, I., Jarvis, D., Varon, D. J., Jacob, D. J., Randles, C. A., Gautam, R., Omara, M., Schade, G. W., Dennison, P.E., Franksberg, C., Gordon, D., Lopinto, E., Miller, C. E. (2020). Multisatellite imaging of a gas well blowout enables quantification of total methane emissions. *Geophysical Research Letters*, 48(2), Article Number [e2020GL09086]. <https://doi.org/10.1029/2020GL090864>
- Equinor ASA. (2019, August 15) *Mariner on stream*. equinor. <https://www.equinor.com/news/archive/2019-08-mariner>
- Foote, M. D., Dennison, P. E., Thorpe, A. K., Thompson, D. R., Jongaramrungruang, S., Frankenberg, C., & Joshi, S. C. (2020). Fast and Accurate Retrieval of Methane Concentration From Imaging Spectrometer Data Using Sparsity Prior. *IEEE Transactions on Geoscience and Remote Sensing*, 58(9), 6480–6492. <https://doi.org/10.1109/TGRS.2020.2976888>
- Cenovus Energy, Inc. (2022, May 31). *Cenovus announces restart of West White Rose Project*. Cenovus Energy. <https://www.cenovus.com/News-and-Stories/News-releases/2022/2452998>
- Gorchov Negrón, A. M., Kort, E. A., Conley, S. A., Smith, M. L. (2020). Airborne assessment of methane emissions from offshore platforms in the U.S. Gulf of Mexico. *Environmental Science & Technology*, 54(8), 5112–5120. <https://pubs.acs.org/doi/full/10.1021/acs.est.0c00179>
- Irakulis-Loitxate, Itziar, et al. “Satellites Detect a Methane Ultra-Emission Event from an Offshore Platform in the Gulf of Mexico.” *Environmental Science & Technology Letters*, vol. 9, no. 6, June 2022, pp. 520–25. DOI.org (Crossref), <https://doi.org/10.1021/acs.estlett.2c00225>.
- Kirschke, S., Bousquet, P., Ciais, P., et al., (2013). Three decades of global methane sources and sinks. *Nature Geoscience*, 6, 813-823. 10.1038/ngeo1955
- National Oceanic and Atmospheric Administration data. (2017). *RTMA: Real-time mesoscale analysis*. Google. Retrieved October 1, 2022, from https://developers.google.com/earth-engine/datasets/catalog/NOAA_NWS_RTMA
- Plant, G., Kort E.A., Brandt, A.R., Chen, Y., Fordice, G., Gorchov Negrón, A.M., Schwietzke, S., Smith, M., Zavala-Araiza, D. (2022). Inefficient and unlit natural gas flares both emit large quantities of methane. *Science*. 377(6614), 1566-1571. <https://www.science.org/doi/pdf/10.1126/science.abq0385>
- Short-Term Energy Outlook (STEO). (2019). https://www.eia.gov/outlooks/steo/pdf/steo_full.pdf
- Varon, D. J., Jarvis, D., McKeever, J., Spence, I., Gains, D., Jacob, D. J. (2021). High-frequency monitoring of anomalous methane point sources with multispectral Sentinel-2 satellite observations. *Atmospheric Measurement Techniques*, 14(4), 2771–2785. <https://doi.org/10.5194/amt-14-2771-2021>
- Vaughn, K. (2022, August 22). *Study suggests offshore oil and gas production in Gulf of Mexico has higher methane loss rates than typical onshore production*. Carbon Mapper. <https://carbonmapper.org/study-suggests-offshore-oil-and-gas-production-in-gulf-of-mexico-has-higher-methane-loss-rates-than-typical-onshore-production/>
- Wecht, H. (2022). *BOEM’s greenhouse gas inventory and studies, EPA oil & gas greenhouse gas data webinar*. https://www.epa.gov/system/files/documents/2022-09/ghgi-webinar2022_wecht.pdf
- Xiao, Y., Logan, J. A., Jacob, D. J., Hudman, R. C., Yantosca, R., Blake, D. R. (2008). Global budget of ethane and regional constraints on U.S. sources. *Journal of Geophysical Research Atmospheres*, 113(D21), Article Number [D21306]. <https://doi.org/10.1029/2007JD009415>

- Zeringue, B. A., Hahn, M. B., Riches, T. J., De Cort, T. M., Maclay, D. M., Wilson, M. G. (2022) *U.S. Outer Continental Shelf Gulf of Mexico Region Oil and Gas Production Forecast: 2022 – 2031*. United States Department of the Interior Bureau of Ocean Energy Management Gulf of Mexico, OCS Region New Orleans Office of Resource Evaluation. <https://www.boem.gov/sites/default/files/documents/regions/gulf-mexico-ocs-region/US%20OCS%20GOMR%20Oil%20and%20Gas%20Production%20Forecast%202022-2031.pdf>
- Zhang, Y., Gautam, R., Zavala-Araiza, D., Jacob D. J., Zhang, R., Sheng, J. Scarpetti, T. (2019). Satellite-observed changes in Mexico's offshore gas flaring activity to oil/gas regulations. *Geophysical Research Letters*, 46(3), 1879-1885. <https://doi.org/10.1029/2018GL081145>

9. Appendices

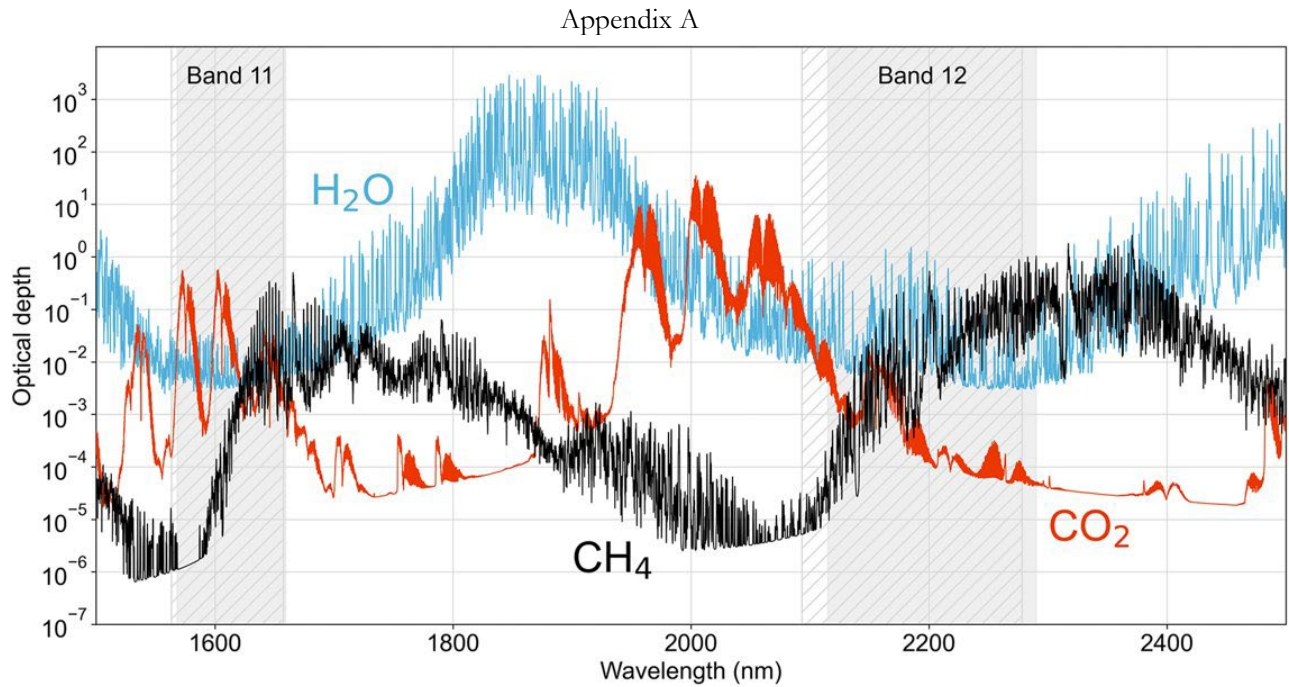


Figure A1: Methane (CH₄), CO₂, and water vapor (H₂O) slant column optical depths in the 1500–2500 nm SWIR spectral range. Values are for the US Standard Atmosphere. The gray shaded areas are the spectral ranges of bands 11 and 12 for Sentinel-2A (solid) and Sentinel-2B (hatched). (Varon et al. 2021)

Appendix B

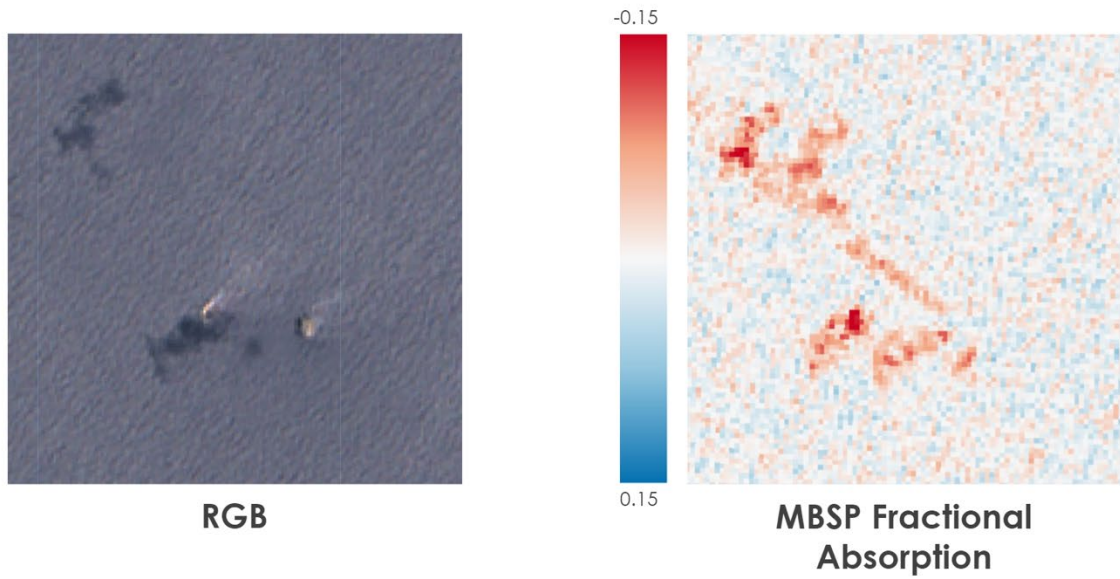


Figure B1: RGB image of “Constitution” platform, as seen in Google Earth Engine (left); MBSP fractional absorption layer as seen in Google Earth Engine.

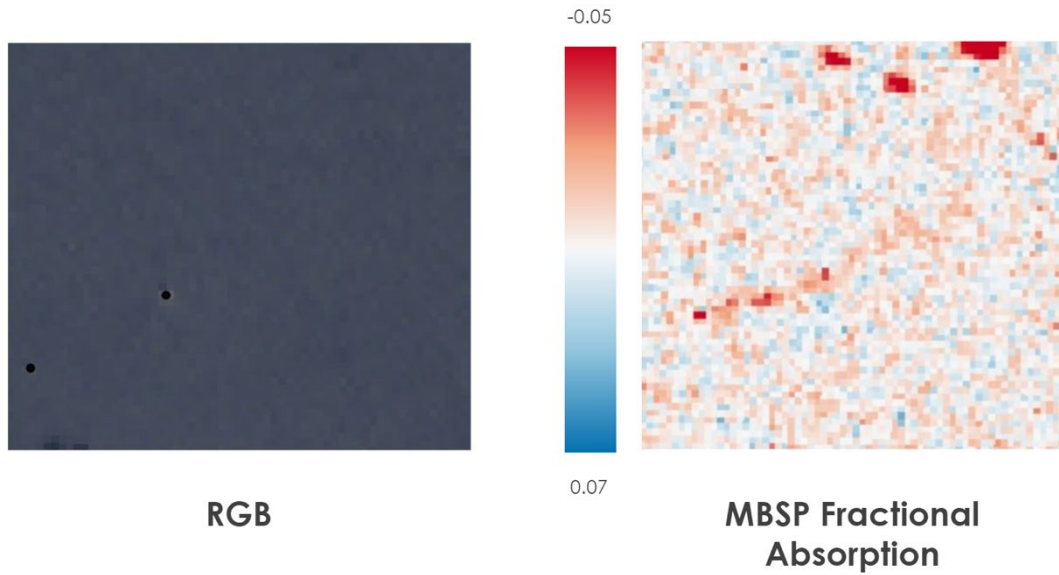


Figure B2: RGB image of "F" platform, as seen in Google Earth Engine (left). Black dots represent platform locations as logged in BOEM data center; MBSP fractional absorption layer as seen in Google Earth Engine.

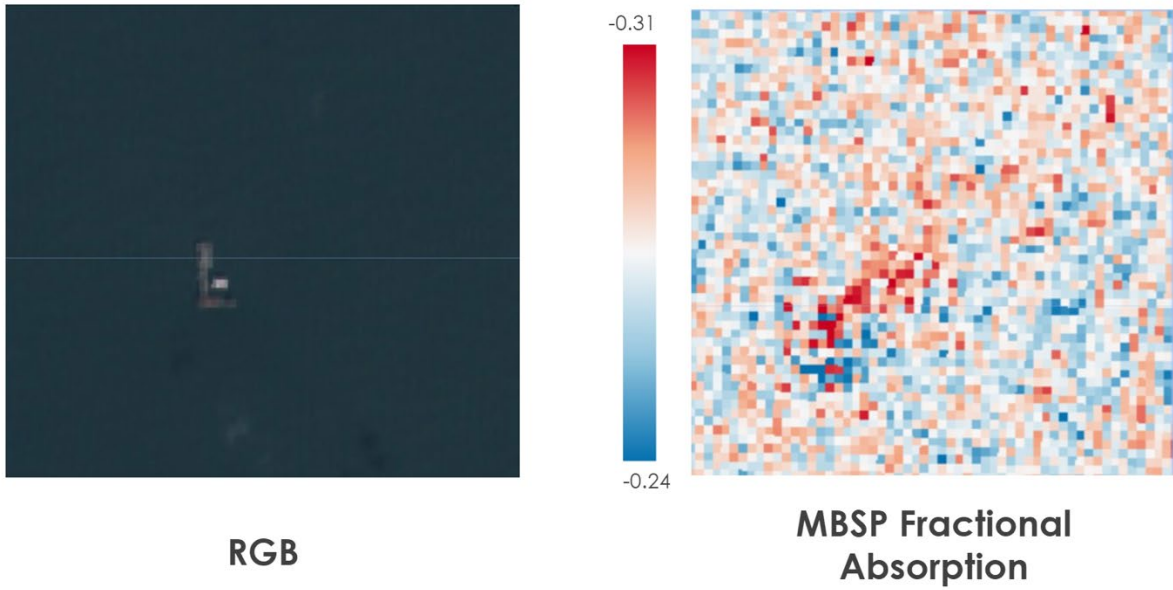


Figure B3: RGB image of "PRD" platform, as seen in Google Earth Engine (left); MBSP fractional absorption layer as seen in Google Earth Engine.

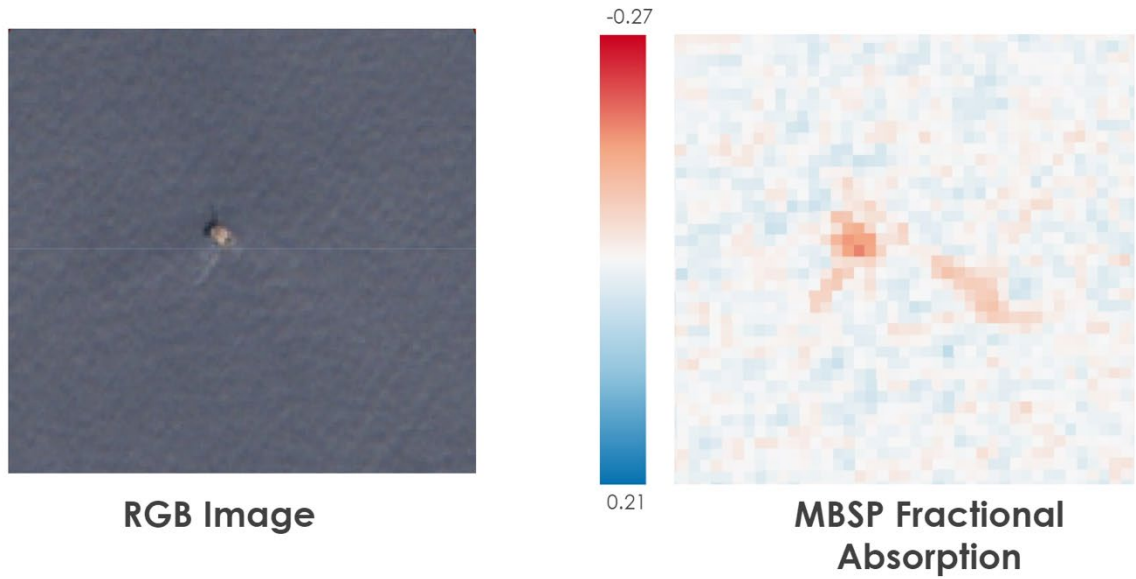


Figure B4: RGB image of "Petronius" platform, as seen in Google Earth Engine (left); MBSP fractional absorption layer as seen in Google Earth Engine.